Shifts with temperature of the EPR signal in Cu(L-alanine)$_2$: A low-dimensional paramagnet

Rafael Calvo and Mario C. G. Passeggi
Instituto de Desarrollo Tecnológico para la Industria Química (INTEC), Güemes 3450, 3000 Santa Fe, Argentina
(Received 12 October 1990; revised manuscript received 18 March 1991)

EPR measurements of the temperature dependence of the g factor have been performed on single crystals of Cu(L-alanine)$_2$, the copper complex of the amino acid L-alanine. The angular variation of the observed g-value shifts reflects the layered arrangement of the copper ions in the crystal structure of this compound. The experimental results are interpreted in terms of the theory of Kubo and Tomita for the magnetic resonance absorption. Using only parameters obtained from the EPR data and crystallographic information for Cu(L-alanine)$_2$, it is shown that the dominant contribution to the temperature dependent g-value shifts arises from the combined effect of the dipole-dipole interaction between copper ions and the spin polarization induced by the applied magnetic field. The effect of this first-order mechanism is independent of the Heisenberg exchange ($J/k \approx -0.5$ K) and the spin dynamics of the system, and predicts an angular dependence and magnitudes for the g-value shifts in good agreement with the data. Our calculations reveal the important role played by the geometry of the spin arrangement in the magnitude and angular variation of the shifts.

I. INTRODUCTION

The temperature (T) dependence of the electron paramagnetic resonance (EPR) absorption spectra in paramagnetic materials can be studied from different points of view. The most direct change is that of the intensity of the resonance, due to the proportionality of the absorption to the T-dependent (static) magnetic susceptibility. However, absolute measurements of the EPR absorption intensity as a function of T are rather difficult to perform. Easier to follow are changes in the shape, position, and linewidth of the resonances. Lattice expansion and structural phase transitions, as well as spin-lattice relaxation effects, produce variations in the local internal fields "seen" by the spins, then inducing changes with T in the overall magnetic response of the system. In the case of thermal expansion, the changes are larger at higher temperatures. Spin-lattice relaxation also causes a broadening of the resonances when T is increased.

In this work we study changes with T of the positions of the resonances arising from the polarization of the spin system. These changes are larger at lower T. The problem has been studied by Kambe and Usui,[1] who obtained the moments of any order of the spectra as a function of T and reported explicit results for the zeroth-, first-, and second-order moments. They calculated the changes with T in the positions and shapes of the resonances and applied the results to the cases of EPR for noninteracting and equivalent magnetic ions, as well as NMR in (electronic) paramagnetic crystals.

McMillan and Opechowski[2] analyzed in detail the T dependence of the positions and shapes of the resonances in cases where the spin-spin interactions are not negligible. Their results were applied to systems with effective spins $\frac{1}{2}$ and 1 and illustrated with data for nickel fluosilicate.

Nagata and Tazuke[3] calculated the effect of short-range order on the positions of the EPR signals in the linear-chain antiferromagnets $CsMnCl_3 \cdot 2H_2O$ and $(CH_3)_4NMnCL_3$. The one-dimensional (1D) behavior of the spin dynamics of these materials, where the Mn^{2+} ions are arranged in chains, allowed these authors to use the spin-correlation functions obtained from Fisher's exact solution[4] for the classical 1D antiferromagnet. Considering a situation in which the Zeeman energy is larger than the dipolar energy, but smaller than the isotropic exchange energy, Nagata and Tazuke[3] obtained good agreement between the predicted and observed T variations of the gyromagnetic factor. Small discrepancies were attributed to fine-structure terms, which are important for Mn^{2+} ($S=\frac{5}{2}$) ions.

In recent EPR studies of a series of paramagnetic copper–amino acid complexes [Cu(AA)$_2$], we have observed sizable changes with temperature in the positions of the EPR resonances. Preliminary experimental results[5,6] were analyzed in terms of a phenomenological model, and the magnitude and angular variation of the changes with T were qualitatively related to the layered arrangement of the copper ions in Cu(AA)$_2$.[6,7] Here we report EPR data in single crystals of the copper derivative of the amino acid L-alanine $Cu[NH_2CHCH_3CO_2]_2$, to be called Cu (L-alanine)$_2$, obtained at 9 GHz, as a function of temperature between 1.5 and 293 K. A large and anisotropic temperature variation in the line position is observed for $T \leq 50$ K, i.e., at temperatures where magnetic order due to exchange coupling ($J/k \approx = 0.5$ K) is not expected. To explain the data we use a theory based on the linear response formalism and the Anderson-Kubo theory[8,9] for the magnetic resonance absorption, which considers the polarization of the spin system induced by the external magnetic field when the temperature is lowered. Because of the dipole-dipole interaction be-

tween spins, this polarization, which becomes effective in low-dimensional systems, gives rise to a net internal field, shifting the resonance line. Using only measurable parameters (structural data, g tensors), the model predicts well the general characteristics of the data. Corrections to the model arising from anisotropic exchange or from higher-order mechanisms, which depend on the exchange interaction and spin dynamics, are of little importance for $Cu(AA)_2$ because of the relative smallness of J. Consequently, the general trends predicted by our model for the T dependence of the line positions are particularly applicable to systems where the exchange interactions are small and comparable to the Zeeman interaction, as observed in Cu(L-alanine)$_2$.

II. COPPER–AMINO ACID COMPLEXES AND Cu (L-alanine)$_2$

Different experimental techniques have been used to study the magnetic properties of $Cu(AA)_2$. Because of the layered arrangement of the copper ions in their crystal structures, most $Cu(AA)_2$ exhibits low-dimensional magnetic behavior. This has been shown through magnetic susceptibility[10,11] and electron paramagnetic resonance (EPR) on single-crystal samples,[11–15] as well as by specific-heat measurements.[16] EPR has been shown to be an appropriate tool to reveal the low-dimensional magnetic behavior of these compounds. As an example, selective collapse of the resonances of magnetically nonequivalent spins within a copper layer in Cu(L-isoleucine)$_2$ occurs as a result of the magnitude of the intralayer exchange interaction.[14] No such collapse occurs for the resonance lines corresponding to spins in different layers, indicating a difference in magnitudes between the intra- and interlayer exchange interaction. Also, linewidth data in some $Cu(AA)_2$ can be interpreted in terms of the theory developed by Richards and Salamon,[17,18] which considers the effect of the spin dynamics on the dipole-dipole interactions in 2D spin systems.

The x-ray crystal structure of Cu (L-alanine)$_2$ was reported by Dijkstra[19] and more recently by Hitchman *et al.*[20] It is monoclinic, corresponding to the space group $P2_1$, with $a=9.166$ Å, $b=5.045$ Å, $c=9.521$ Å, and $\beta=94.6°$. There are two species (A and B) of symmetry-related copper atoms, which are arranged in layers parallel to the b-c plane, at distances 5.05 and 5.39 Å between nearest-neighbor coppers within the layers and 9.14 Å between layers.

Our magnetic-susceptibility measurements, between 0.013 and 240 K in powders of Cu (L-alanine)$_2$,[11] suggested a predominant spin-chain behavior with an antiferromagnetic exchange interaction $J/k=-0.52$ K, between nearest-neighbor copper ions. On the other hand, the observed change of the EPR linewidth with the microwave frequency[11] was attributed to the presence of two nonequivalent lattice sites for copper in Cu(L-alanine)$_2$. The linewidth data and a model[15,21] based on the theory of Kubo and Tomita for the magnetic-resonance absorption, allowed us to calculate $|J|/k=0.47$ K for the exchange parameter.[11] The agreement between these two values of J, obtained from different experiments, indicated a predominantly 1D exchange network in Cu(L-alanine)$_2$.

III. EXPERIMENTAL DETAILS AND RESULTS

The procedures followed to grow and orient single-crystal samples of Cu(L-alanine)$_2$ have been described in Ref. 11. The samples used in this work were thin plates of about $0.1\times2\times4$ mm^3. We used an E-12 Varian EPR spectrometer having a rotating 12-in. magnet with Hall-probe control and a cylindrical cavity[22] cooled within a conventional set of nitrogen and helium Dewars.

The temperature of the sample, measured with calibrated copper and carbon resistors, was maintained at fixed points (293, 77, 4, and 1.5 K), while the angular variations of the line position were measured in three perpendicular planes a'-b, a'-c, and b-c, where $\hat{\mathbf{a}}'=\hat{\mathbf{b}}\times\hat{\mathbf{c}}$. In other sets of experiments, the magnetic field was oriented along the crystal axes $\hat{\mathbf{a}}'$, $\hat{\mathbf{b}}$, and $\hat{\mathbf{c}}$, and the line position was measured as a function of T as T was slowly varied between 1.5 and 293 K. A single, exchange-collapsed EPR line was observed in all cases for the two nonequivalent copper sites in Cu(L-alanine)$_2$. The g factor was obtained using a microwave-frequency counter and a NMR fluxmeter to measure the magnetic field. The angular variation of the squared g factor measured in the b-c. a'-b, and a'-c crystal planes, at 293, 77, 4, and 1.5 K, is displayed in Fig. 1. The g factor increases with decreasing T when the magnetic field $\mathbf{B}$ is applied in the b-c crystal plane (where the copper layers are located), while it decreases when $\mathbf{B}$ lies along the $\hat{\mathbf{a}}'$ axis normal to this plane. The temperature dependence of the g factor observed for $\mathbf{B}$ applied along the $\hat{\mathbf{a}}'$, $\hat{\mathbf{b}}$, and $\hat{\mathbf{c}}$ axes is displayed in Fig. 2 as a function of $1/T$. Below 50 K, g is proportional to $1/T$ for all directions of $\mathbf{B}$.

IV. ANALYSIS OF THE DATA

The data in Figs. 1 and 2 were analyzed using a spin Hamiltonian and a phenomenological model that helps to stress the observed features and tabulate the experimental results. It defines the g tensor $\overleftrightarrow{g}_0$ measured at high T as

$$\mathcal{H}=\mu_0\mathbf{S}\cdot\overleftrightarrow{g}_0\cdot\mathbf{B}\ , \tag{1}$$

where $\mathbf{S}$ is the effective spin ($S=\frac{1}{2}$) and μ_0 is the Bohr magneton. When T is lowered, the effective field acting on the spins is the sum of $\mathbf{B}$ and an internal field $\mathbf{B}_{\rm int}$ produced by the polarized neighbor spins. Then

$$\mathcal{H}_T=\mu_0\mathbf{S}\cdot\overleftrightarrow{g}_0\cdot[\mathbf{B}+\mathbf{B}_{\rm int}(T)]\ , \tag{2}$$

where $\mathbf{B}_{\rm int}(T)\rightarrow0$ for $T\rightarrow\infty$. We assume a tensorial (linear) dependence between $\mathbf{B}_{\rm int}$ and $\mathbf{B}$ given by

$$\mathbf{B}_{\rm int}(T)=4\pi\overleftrightarrow{\chi}(T)\cdot\mathbf{B}\ , \tag{3}$$

where the "internal susceptibility" tensor $\overleftrightarrow{\chi}(T)$ has to be real and symmetric.[23] Then

$$\mathcal{H}_T=\mu_0\mathbf{S}\cdot\overleftrightarrow{g}_T\cdot\mathbf{B}\ , \tag{4}$$

where

$$\vec{\vec{g}}_T=[\vec{\vec{U}}+4\pi\vec{\vec{\chi}}(T)]\cdot\vec{\vec{g}}_0 \ . \tag{5}$$

In Eq. (5), $\vec{\vec{g}}_0$ is assumed to be the limiting value of $\vec{\vec{g}}_T$ for T large and $\vec{\vec{U}}$ is the unit matrix. The components of the symmetric tensors $\vec{\vec{g}}_T^2$ and $\vec{\vec{g}}_0^2$ were evaluated from the data at different T displayed in Fig. 1, by least-squares fitting to the function

$$\begin{aligned} g_T^2(\theta,\Phi)=&(g_T^2)_{xx}\sin^2\theta\cos^2\Phi+(g_T^2)_{yy}\sin^2\theta\sin^2\Phi \\ &+(g_T^2)_{zz}\cos^2\theta+(g_T^2)_{xy}\sin^2\theta\sin\Phi\cos\Phi \\ &+(g_T^2)_{zx}\sin\theta\cos\theta\cos\Phi \\ &+(g_T^2)_{zy}\sin\theta\cos\theta\sin\Phi \ . \end{aligned} \tag{6}$$

The polar and azimuthal angles θ and Φ in Eq. (6) are defined in an x,y,z axes system when $\hat{x}=\hat{a}'$, $\hat{y}=\hat{b}$, and $\hat{z}=\hat{c}$.

The values obtained for the components of $\vec{\vec{g}}_T^2$ are given in Table I. The components $(g_T^2)_{xy}$ and $g_T^2)_{zy}$ are zero at any T, as expected from the symmetry of Cu(*L*-alanine)$_2$.

Figure 2 shows the linear relation between the g factor and reciprocal temperature ($1/T$) observed for all directions of **B**, in the low-T region, i.e.,

$$g_\alpha(T)=A_\alpha+B_\alpha/T \ . \tag{7}$$

Least-squares fits of Eq. (7) to values of $g_\alpha(T)$ observed for $\hat{\alpha}=\hat{a}'$, $\hat{b}$, and $\hat{c}$ were performed, and the results are included in Fig. 2 and Table II. Above 50 K the devia-

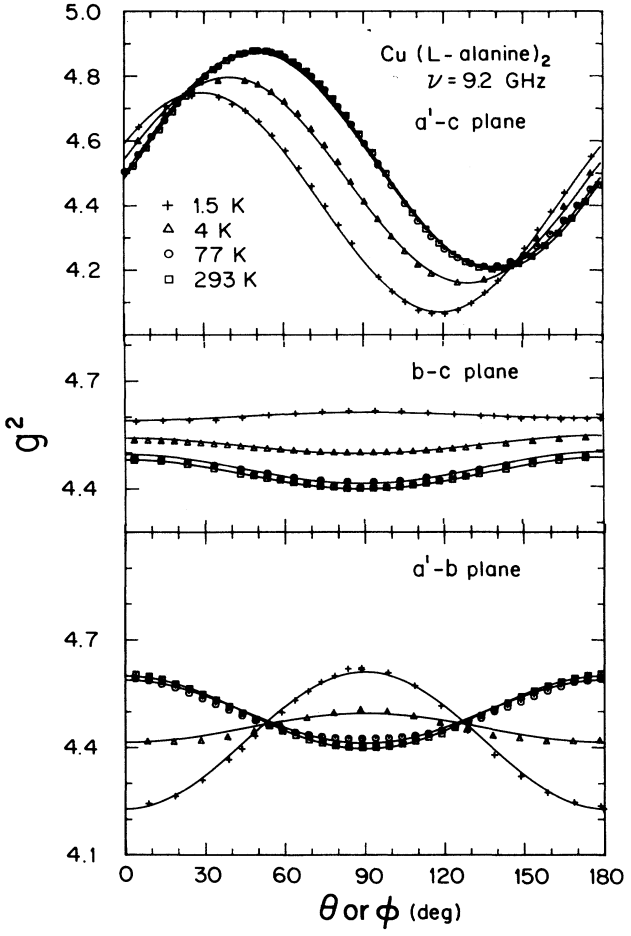

FIG. 1. Angular variation of the g factor measured in the three crystallographic planes at fixed temperatures. The solid lines are the best fits to Eq. (6) and were obtained with the components of the tensor $\vec{\vec{g}}_T^2$ given in Table I.

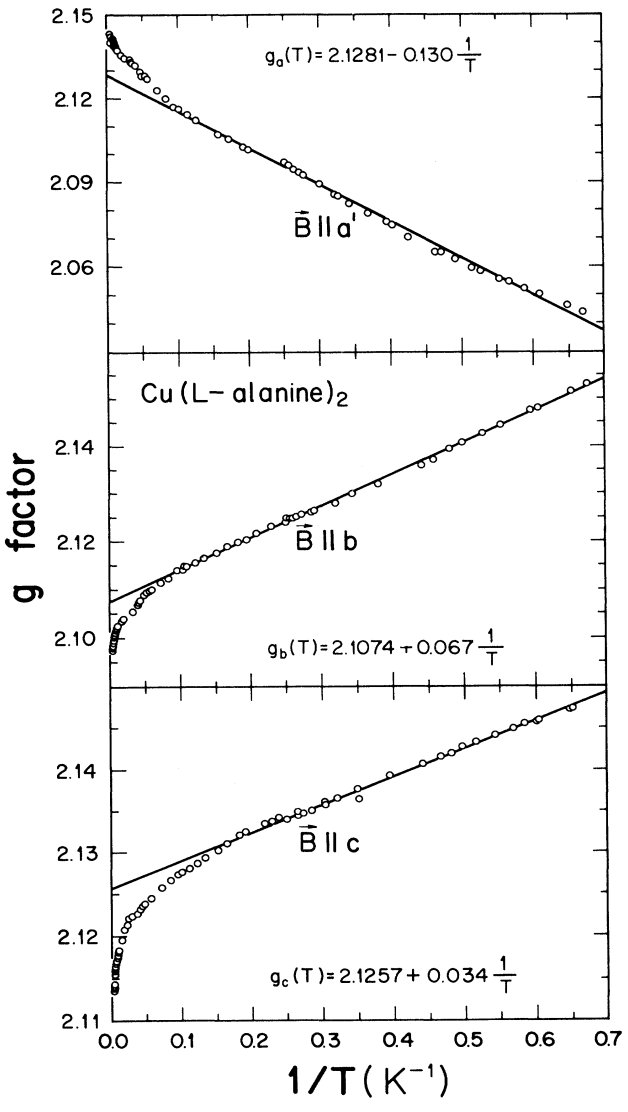

FIG. 2. Temperature dependence of the g factor measured for fields applied along the $\hat{a}'=\hat{b}\times\hat{c}$, $\hat{b}$, and $\hat{c}$ crystal axes. The data are plotted as a function of inverse temperature to show the linear behavior observed at low T. Least-squares fits of the data to Eq. (5) are included.

TABLE I. Components $(g_T^2)_{ij}$ of the gyromagnetic tensor obtained by least-squares fits of Eq. (6) to the data in Fig. 1, obtained at 9 GHz, at different temperatures T. The components $(g_T^2)_{zy}$ and $(g_T^2)_{xy}$ are zero because of the lattice symmetry of Cu(L-alanine)$_2$. The uncertainties are calculated from the dispersion of the data. The values indicated as for $T=\infty$ were obtained from the extrapolation of the low-T data.

T (K)	293	77	4	1.5	∞
$(g_T^2)_{xx}$	4.599(1)	4.587(2)	4.415(2)	4.229(2)	4.529
$(g_T^2)_{yy}$	4.396(1)	4.412(2)	4.495(2)	4.609(2)	4.441
$(g_T^2)_{zz}$	4.481(1)	4.496(1)	4.542(2)	4.590(2)	4.519
$(g_T^2)_{zx}$	0.334(1)	0.330(2)	0.312(2)	0.287(2)	0.326

tions form the $1/T$ dependence are large, probably because of lattice expansion effects. Thus only experimental results below 10 K were considered in performing the fits.

The components of the tensor $\overleftrightarrow{g}_0^2$, included in Table I, were obtained from an extrapolation to high T ($1/T\rightarrow 0$), of the low-temperature data displayed in Fig. 2 and from the parameters obtained from the fits with Eq. (7). The components of $\overleftrightarrow{g}_0$ were then obtained from those of $\overleftrightarrow{g}_0^2$, assuming that $\overleftrightarrow{g}_0$ is symmetric.[24] Using Eq. (5), and since $\overleftrightarrow{g}_T^2$ is also a symmetric tensor, it is

$$\overleftrightarrow{g}_T^2-\overleftrightarrow{g}_0^2\approx 8\pi\overleftrightarrow{g}_0\cdot\overleftrightarrow{\chi}(T)\cdot\overleftrightarrow{g}_0 . \tag{8}$$

Considering Eq. (8), the components of the tensor $\overleftrightarrow{\chi}(T)$ can be obtained from the experimental data at different T, using

$$\overleftrightarrow{\chi}(T)=\frac{1}{8\pi}\overleftrightarrow{g}_0^{-1}\cdot(\overleftrightarrow{g}_T^2-\overleftrightarrow{g}_0^2)\cdot\overleftrightarrow{g}_0^{-1}=\frac{\overleftrightarrow{C}}{T} . \tag{9}$$

According to the $1/T$ temperature dependence of the g factor shown by Fig. 2, the tensor $\overleftrightarrow{C}=T\overleftrightarrow{\chi}(T)$ defined in Eq. (9) is symmetric and T independent. Its components are given in Table II, where the values of A_α and B_α are included.

TABLE II. Values of the parameters A_α and B_α for $\hat{\alpha}=\hat{\mathbf{x}}$, $\hat{\mathbf{y}}$, $\hat{\mathbf{z}}$ (where $\hat{\mathbf{x}}=\hat{\mathbf{a}}'=\hat{\mathbf{b}}\times\hat{\mathbf{c}}$, $\hat{\mathbf{y}}=\hat{\mathbf{b}}$, and $\hat{\mathbf{z}}=\hat{\mathbf{c}}$), obtained by least-squares fits of Eq. (7) to the data in Fig. 2. Values of the components of the tensor $\overleftrightarrow{C}$, defined in Eq. (9), obtained from the data in Figs. 1 and 2, and those calculated with our model, as described in the text.

Parameter	Experimental	Calculated
A_x	2.1281	
B_x	−0.13 K	−0.086 K
A_y	2.1074	
B_y	0.067 K	0.051 K
A_z	2.1257	
B_z	0.034 K	0.035 K
C_{xx}	-3.93×10^{-3} K	-3.23×10^{-3} K
C_{yy}	2.25×10^{-3} K	1.91×10^{-3} K
C_{zz}	0.97×10^{-3} K	1.32×10^{-3} K
C_{zx}	-0.41×10^{-3} K	-0.11×10^{-3} K

V. TEMPERATURE VARIATION OF THE EPR ABSORPTION

A. Magnetic resonance absorption in the high-T limit

Within the linear-response theory, the EPR spectra at low microwave powers are described by the absorption component of the dynamical susceptibility $\chi''(\omega)$:[8,9,25–27]

$$\chi''(\omega)=\frac{\omega V}{2kT}\int_{-\infty}^{\infty}\langle M_\sigma(t)M_\sigma\rangle\exp(-i\omega t)dt . \tag{10}$$

In Eq. (10), M_σ is the component of the magnetic moment for unit volume of the sample (magnetization operator) along the linearly polarized rf field $\mathbf{B}_1$ ($\hat{\sigma}=\mathbf{B}_1/|\mathbf{B}_1|$), having a frequency ω. Equation (19) is valid provided that $\hbar\omega\ll kT$.

For a system of N equivalent isotropic spins $\mathbf{S}_i$ per unit volume, the magnetization operator is given by

$$\mathbf{M}=-g\mu_0\sum_{i=1}^{N}\mathbf{S}_i=-g\mu_0\mathbf{S} , \tag{11}$$

where $\mathbf{S}$ is the total spin. The operator $M_\sigma(t)$ in Eq. (10) is

$$M_\sigma(t)=\exp(i\mathcal{H}t/\hbar)M_\sigma\exp(-i\mathcal{H}t/\hbar) , \tag{12}$$

where $\mathcal{H}$ is the full Hamiltonian of the spin system. The thermal average

$$\langle M_\sigma(t)M_\sigma\rangle=\mathrm{Tr}[\rho M_\sigma(t)M_\sigma] \tag{13}$$

is calculated with the density matrix

$$\rho=\exp(-\mathcal{H}/kT)/\mathrm{Tr}[\exp(-\mathcal{H}/kT)] . \tag{14}$$

The magnetization $\mathbf{M}$ interacts with the static magnetic field $\mathbf{B}$, and the Zeeman Hamiltonian is given by

$$\mathcal{H}_z=-\mathbf{M}\cdot\mathbf{B}=g\mu_0\mathbf{S}\cdot\mathbf{B} . \tag{15}$$

The dipole-dipole interaction between isotropic spins is given by

$$\mathcal{H}_{\mathrm{dd}}=\frac{1}{2}{\sum_{i,j}}'\frac{g^2\mu_0^2}{R_{ij}^3}[\mathbf{S}_i\cdot\mathbf{S}_j-3(\mathbf{S}_i\cdot\hat{\mathbf{R}}_{ij})(\mathbf{S}_j\cdot\hat{\mathbf{R}}_{ij})] , \tag{16}$$

where $\mathbf{R}_{ij}=\mathbf{R}_i-\mathbf{R}_j$ is the vector joining the spins at $\mathbf{R}_i$ and $\mathbf{R}_j$, and $\hat{\mathbf{R}}=\mathbf{R}/|\mathbf{R}|$. The case of the dipole-dipole interaction for anisotropic spins is analyzed in the Appen-

dix, using existing methods.[28] Another contribution to the Hamiltonian $\mathcal{H}$ is the isotropic exchange interaction

$$\mathcal{H}_{ex}=-\sum_{i,j} J_{ij}\mathbf{S}_i\cdot\mathbf{S}_j \quad (J_{ii}=0) , \tag{17}$$

where the sum is over all spin pairs. Anisotropic (symmetric and antisymmetric) exchange interactions,[29] as well as hyperfine interactions, may contribute to the Hamiltonian $\mathcal{H}$ and are considered in the Appendix.

It is seen in Eq. (15)–(17) that $[\mathcal{H}_z,\mathcal{H}_{ex}]=0$, but $[\mathcal{H}_z,\mathcal{H}_{dd}]$ and $[\mathcal{H}_{ex},\mathcal{H}_{dd}]$ are nonzero. Considering that $\mathcal{H}_{dd}$ has a magnitude smaller than $\mathcal{H}_z$ and $\mathcal{H}_{ex}$, the standard procedure to calculate the EPR spectrum from Eq. (10) is a perturbative method,[8,9,25,26] which separates the Hamiltonian $\mathcal{H}$ as

$$\mathcal{H}=\mathcal{H}_z+\mathcal{H}_{ex}+\mathcal{H}_{dd}=\mathcal{H}_0+\mathcal{H}' , \tag{18}$$

where

$$\mathcal{H}_0=\mathcal{H}_z+\mathcal{H}_{ex} \tag{19}$$

is the unperturbed Hamiltonian and, in the simple case we are considering,

$$\mathcal{H}'=\mathcal{H}_{dd} \tag{20}$$

is the perturbation. The problem is expressed in the base where $\hat{\mathbf{z}}$ is along the applied field $\mathbf{B}$ and $\mathcal{H}_0$ is diagonal. Up to second order in $\mathcal{H}'$ and considering only the resonance at positive frequencies,

$$\chi''(\omega-\omega_0)\approx\frac{\omega V}{2kT}\langle M_+M_-\rangle \times\int_{-\infty}^{\infty}\left[1+i\delta t-\int_0^t\Omega_T(t,\tau)d\tau\right] \times e^{-i(\omega-\omega_0)t}dt , \tag{21}$$

where $\omega_0=g\mu_0B/\hbar$, while

$$\delta=\frac{1}{\hbar}\frac{\langle[\mathcal{H}',S_+]S_-\rangle}{\langle S_+S_-\rangle} \tag{22}$$

and

$$\Omega_T(t,\tau)=\frac{(t-\tau)}{\hbar^2}\frac{\langle[\mathcal{H}',[\mathcal{H}'(\tau),S_+]S_-]\rangle}{\langle S_+S_-\rangle} . \tag{23}$$

In Eq. (23),

$$\mathcal{H}'(\tau)=\exp(i\mathcal{H}_0\tau/\hbar)\mathcal{H}'\exp(-i\mathcal{H}_0\tau/\hbar)$$

is the interaction $\mathcal{H}'$ of Eq. (20), time modulated by the exchange and Zeeman interactions contained in $\mathcal{H}_0$ of Eq. (19). Smaller contributions to Eq. (23), depending on the direction of the microwave field, which appear in systems with a low-symmetry arrangement of spins,[30] are neglected. Within this perturbative scheme, the statistical averages included in Eqs. (21)–(23) can be approximated by using $\mathcal{H}_0$, instead of $\mathcal{H}$ in Eq. (14). At infinite temperature (when $kT\gg g\mu_0B$ and $kT\gg J$), ρ of Eq. (14) is given by

$$\rho\approx\rho_0=\vec{U}/\mathrm{Tr}(\vec{U}) . \tag{24}$$

In this case $\delta=0$, as a well-known result[8,9,25,26] which follows from Eq. (22) using Eq. (24). Also, $\Omega(t,\tau)=\Omega_T(t,\tau)|_{T\to\infty}$ is given by

$$\Omega(t,\tau)=(1/\hbar^2)(t-\tau)\frac{\mathrm{Tr}\{[\mathcal{H}'(\tau),S_+][S_-,\mathcal{H}']\}}{\mathrm{Tr}(S_+S_-)} . \tag{25}$$

When Eq. (25) is introduced in Eq. (21), we obtain the EPR absorption signal at higher temperatures. In the theory introduced by Kubo and Tomita,[9] the terms within the large parentheses of Eq. (21) are considered as arising from the series expansion in powers of $\mathcal{H}'$ of the so-called relaxation function, which at high T (when $\delta=0$) is given by

$$\Phi(t)=\left[1-\int_0^t\Omega(t,\tau)d\tau+\cdots\right] \approx\exp\left[-\int_0^t\Omega(t,\tau)d\tau\right] . \tag{26}$$

Then Eqs. (21) and (26) give

$$\chi''(\omega-\omega_0)=(\omega V/2kT)\mathrm{Tr}(M_+M_-) \times\int_{-\infty}^{\infty}\{\Phi(t)\exp[-i(\omega-\omega_0)t]\}dt , \tag{27}$$

where $\omega_0=g_0\mu_0B/\hbar$. If $\mathcal{H}'$ is neglected, $\Phi(t)=1$, and the spectrum consists of two narrow resonances at $\pm\omega_0$. When $\mathcal{H}'$ is considered, there are two kinds of contributions. Secular contributions to $\Omega(t,\tau)$ (those arising from the terms of $\mathcal{H}'$ commuting with $\mathcal{H}_z$) give rise to broadening of the line. Nonsecular terms produce shifts of the resonances, as well as additional contributions to the linewidth. Both broadening and shifts of the lines involve the presence of $\mathcal{H}_{ex}$ through the phenomenon of exchange narrowing.[8,9] As mentioned above, besides $\mathcal{H}_{dd}$, other contributions to $\mathcal{H}'$ of Eq. (20) may add similar effects which have been discussed by different authors.[18,25,26,31,32]

B. Temperature dependence of the absorption

The $T\to\infty$ approximation [Eq. (24)] leading from Eqs. (21)–(23) to Eq. (27) enters through the values of $\langle M_+M_-\rangle$, $\delta=0$, and $\Omega_T(t,\tau)=\Omega(t,\tau)$. At finite temperatures the T dependence of $\langle M_+M_-\rangle$ is proportional to the static susceptibility and varies accordingly with T, producing a change in the signal intensity, which is not considered here. The thermal averages involved in δ and $\Omega_T(t,\tau)$ in Eqs. (22) and (23) may be calculated at finite but high temperatures by a series expansion in $1/kT$. Then, at finite T, $\Phi(t)$ of Eq. (26) should be replaced by

$$\Phi'(t)=\left[1+i\delta t-\int_0^t\Omega(t,\tau)d\tau+\cdots\right] \approx\Phi(t)\exp(i\delta t) , \tag{28}$$

where we have neglected finite-temperature corrections in $\Omega_T(t,\tau)$ and δ is given by

$$\delta=-\mathrm{Tr}(\mathcal{H}_0[\mathcal{H}',S_+]S_-)/[\mathrm{Tr}(S_+S_-)\hbar kT] . \tag{29}$$

When $\Phi'(t)$ of Eq. (28) replaces $\Phi(t)$ of Eq. (26) and is introduced in Eq. (27), it gives

$$\chi''(\omega-\omega_0)=(\omega V/2kT)\langle M_+M_-\rangle \times\int_{-\infty}^{\infty}\exp\{-i[\omega-(\omega_0+\delta)]t\}\Phi(t)dt \ . \quad (30)$$

Therefore, δ represents a frequency shift in the position ω_0 of the resonance line. Thus we may define an effective temperature-dependent g factor $g(T)$ as

$$g(T)=\hbar(\omega_0+\delta)/\mu_0 B =g_0\left[1-\frac{\mathrm{Tr}(S_z[\mathcal{H}',S_+]S_-)}{kT\,\mathrm{Tr}(S_+S_-)}\right] . \quad (31)$$

If $\mathcal{H}'$ consists only on the dipole-dipole interaction between isotopic spins [$\mathcal{H}_{dd}$ of Eq. (16)], one gets, from Eq. (31) and Eqs. (A17)–(A19) of the Appendix,

$$\frac{g^2(T)-g_0^2}{g_0^2}=\frac{-3g_0^2\mu_0^2}{4kT}\sum_i\frac{1-3(\hat{\mathbf{b}}\cdot\hat{\mathbf{R}}_{0i})^2}{R_{0i}^3} , \quad (32)$$

where $\hat{b}=\mathbf{B}/|\mathbf{B}|$ is the direction of the applied field $\mathbf{B}$. The sum in Eq. (32) assumes that one spin is located at the origin of coordinates.

It should be noted that the theory developed up to this point makes use of an expansion up to first order in two different senses. On the one hand, it involves a first-order correction in $\mathcal{H}_0/kT$ for the density matrix used to calculate the thermal averages. On the other hand, it is linear in the perturbation $\mathcal{H}'$. Taking into account that $\mathcal{H}_0=\mathcal{H}_z+\mathcal{H}_{ex}$ and $\mathcal{H}'$ are traceless and because of the isotropy of $\mathcal{H}_{ex}$ in the spin space, only the combination of $\mathcal{H}_z$ and $\mathcal{H}_{dd}$ may create at each lattice point a local field which shifts the resonance. This occurs provided that the symmetry of the spin arrangement allows for $\mathcal{H}_{dd}$ to become effective (shown in Sec. V C). This result is reflected by Eq. (32), which does not depend on the magnitude of the exchange interaction.

Two types of second-order corrections may be considered. The first type arises from terms in $(\mathcal{H}_0/kT)^2$ in the expansion of δ, being still linear in $\mathcal{H}'$. It can be shown that their explicit forms agree with those that can be derived from the results of Nagata and Tazuke[3] who calculated the frequency shifts using the first moment of the resonance line. This is to be expected since, within the theory of Kubo and Tomita,[9] our calculation of $\omega_0+\delta$ amounts essentially to considering the dominant contribution to the first moment. Another type of correction includes that which has $\mathcal{H}'$ to second order, but linear in $\mathcal{H}_0/kT$, which follows from $\Omega_T(t,\tau)$ after expanding Eq. (14) in powers of $1/kT$ in Eq. (23). Both of them involve the presence of the exchange interaction, as might be expected. However, they will not be considered in our treatment on the grounds that, for the system under consideration, $g_0\mu_0 B\sim J\ll kT$ in the range covered by our experiments.

C. Explicit results for simple lattices

In order to discuss our results, we now apply Eq. (32) to simple 1D, 2D, and 3D crystal lattices.

1. 1D chain

In this case, it is $\mathbf{R}_{01}=na\,\hat{\mathbf{e}}_x$ in Eq. (32), where n is an integer, $\hat{\mathbf{e}}_x$ is a unit vector along the chain, and a is the lattice parameter. If θ is the angle between the applied field and chain axis the following is obtained for an infinite chain:

$$S(\theta)\Big|_{1D}=\frac{g^2(T)-g_0^2}{g_0^2}\Big|_{1D}=\frac{-3\alpha K_{1D}}{2T}(1-3\cos^2\theta) , \quad (33)$$

where

$$\alpha=g_0^2\mu_0^2/a^3k \quad (34)$$

and

$$K_{1D}=\sum_{n=1}^{\infty}(1/n)^3\approx 1.202\ldots . \quad (35)$$

For $a\approx 5$ Å and $g=2$, the fractional shift $S(\theta)|_{1D}$ at $T=1$ K is about 7% for $\theta=0$. This value is reduced to a half and changes sign for $\theta=90°$, while it vanishes for $\cos\theta=1/\sqrt{3}$ (the "magic angle" $\theta=54.75°$).

2. 2D square planar lattice

In this case it is

$$\mathbf{R}_{01}=(m\,\hat{\mathbf{e}}_x+n\,\hat{\mathbf{e}}_y)a ,$$

where $\hat{\mathbf{e}}_x$ and $\hat{\mathbf{e}}_y$ are unit vectors in the plane, m and n are integers, and a is the lattice parameter. In this case one obtains

$$S(\theta)\Big|_{2D}=\frac{g^2(T)-g_0^2}{g_0^2}\Big|_{2D}=\frac{3\alpha K_{2D}}{2T}(1-3\cos^2\theta) , \quad (36)$$

where θ is the angle between the applied field and the normal to the spin layer, and

$$K_{2D}=K_{1D}+2\sum_{n,m=1}^{\infty}\frac{n^2}{(m^2+n^2)^{5/2}}=2.244\ldots . \quad (37)$$

Thus a positive shift is expected whenever $\mathbf{B}$ is within the layer ($\theta=90°$), doubling this value and changing sign for $\mathbf{B}$ along the normal to the layer, with a fractional change of about 13% at $\theta=0$, for the same value of α used for the 1D chain and at 1 K. In calculating Eq. (36) it was assumed that there is an infinite (unbounded) layer.

3. 3D simple cubic lattice

Assuming we are dealing with a spherical sample, Eq. (32) vanishes identically in this case.

The previous results for the simplest 1D and 2D spin systems are indicative of the features to be expected for spin arrangements having chain- or layer-type structure. They point to the fact that large temperature variations of the g factor are to be expected for 1D and 2D spin systems and when the real spatial 3D spin configuration approach these ideal cases.

D. Application to the case of Cu(*L*-alanine)$_2$: Contribution of the dipole-dipole interaction

Using the quantization axis $\hat{\mathbf{z}}=\vec{\mathbf{g}}_0\cdot\hat{\mathbf{h}}/|\vec{\mathbf{g}}_0\cdot\hat{\mathbf{h}}|$ as described in the Appendix, it is easy to see from Eqs. (8) and (32) that the tensor $\overleftrightarrow{C}$ in Eq. (9) is, according to our model, given by

$$\overleftrightarrow{C}=-\frac{\mu_0^2}{16\pi k}[3\overleftrightarrow{D}-\overleftrightarrow{U}\mathrm{Tr}\{\overleftrightarrow{D}\}] . \tag{38}$$

Also, the coefficients B_α defined in Eq. (7) are given by [see Eq. (A17)]

$$B_\alpha=\frac{g_0\mu_0^2}{4k}\left[3\frac{\hat{\boldsymbol{\alpha}}\cdot\vec{\mathbf{g}}_0\cdot\overleftrightarrow{D}\cdot\vec{\mathbf{g}}_0\cdot\hat{\boldsymbol{\alpha}}}{\hat{\boldsymbol{\alpha}}\cdot\vec{\mathbf{g}}_0\cdot\vec{\mathbf{g}}_0\cdot\hat{\boldsymbol{\alpha}}}-\mathrm{Tr}(\overleftrightarrow{D})\right] , \tag{39}$$

for $\hat{\boldsymbol{\alpha}}=\hat{\mathbf{x}},\hat{\mathbf{y}},\hat{\mathbf{z}}$. The tensor $\overleftrightarrow{D}$ appearing in Eqs. (38) and (39) is defined in Eqs. (A18) and (A19) of the Appendix.

The components of the symmetry-related tensors $\vec{\mathbf{g}}_A$ and $\vec{\mathbf{g}}_B$, for copper spins in crystal sites A and B in the Cu(*L*-alanine)$_2$ lattice used to calculate the components of $\overleftrightarrow{D}$, were determined from the components of $\vec{\mathbf{g}}_0^2$ (Table I), assuming axial symmetry.[12] The summation in Eq. (A18) was performed numerically, using the crystallographic data for Cu(*L*-alanine)$_2$ reported by Hitchman *et al.*[20] The values of B_α calculated with Eq. (39) are given in Table II, where they are compared with the experimental values. The components of the tensor $\overleftrightarrow{C}$ calculated with Eq. (38) are also given in Table II together with the experimental values. Note that, according to Eq. (38), this tensor should be traceless. In obtaining numerical results we assumed that g_0 in Eq. (39) is obtained from the experiments, although these include small corrections of nonsecular origin.

VI. DISCUSSION

As shown in Table II, the predictions of our model are in good agreement with the values of the components of the tensor $\overleftrightarrow{C}$ calculated from the data. The predicted angular variation of the g-value shifts for the simple case of spins with isotropic g factors in a square planar lattice describes well the behavior of the data displayed in Fig. 1. Equation (38) provides a more appropriate result, in which the structural details of the layered spin arrangement and the anisotropy of the g factor are explicitly included. The discrepancies between these results are relatively small, indicating that the simple model of Sec. V C for the 2D planar lattice contains the physical ingredients most relevant for the case of Cu(*L*-alanine)$_2$.

In a more detailed analysis, the small differences between the calculated and experimental values suggest that other contributions are present. The calculated values of the components of $\overleftrightarrow{C}$, although having the correct sign, have magnitudes smaller than the experimental ones (except for C_{zz}). This indicates that another contribution exists. Since the anisotropic (symmetric) exchange behaves tensorially as the dipole-dipole interaction,[29,32] one is tempted to attribute the discrepancies to this interaction. We have not calculated this contribution to the g-value shifts, which would require knowing the strength of the anisotropic exchange parameters. It is possible to see, however, that anisotropic symmetric exchange is not the only source of discrepancy. According to Eq. (83), both dipole-dipole and anisotropic exchange contributions predict a traceless $\overleftrightarrow{C}$ tensor, in contradiction with the experiments [where $\mathrm{Tr}(\overleftrightarrow{C})=-0.71$ K]. Then additional contributions should be considered, and these can be traced back to the second-order terms in $\mathcal{H}'$, arising from $\Omega_T(t,\tau)$ of Eq. (23). In that case, in addition to $\mathcal{H}_{\mathrm{dd}}$, interactions such as hyperfine, residual Zeeman, etc., can also contribute. Their analyses require the knowledge of the spin-correlation functions of Cu(*L*-alanine)$_2$, which regulate the spin dynamics of the compound.[18,32] These second-order effects in $\mathcal{H}'$ give rise to g-value shifts of nonsecular origins even at $T=\infty$.[33] At finite T they could contribute with a trace of $\overleftrightarrow{C}$ different from zero and become important whenever the correction of first order in $\mathcal{H}'$ and $1/kT$ vanishes, as it could happen because of symmetry reasons.[34]

As a concluding remark, it is interesting to see that the main features of the angular variation of the shifts of g with temperature can be explained through the role played by the 2D spatial arrangement of the magnetic ions, as described through the effect of the dipole-dipole interaction. The time-dependent spin-correlation functions have no role in the shifts with T in the resonance positions of Cu(*L*-alanine)$_2$. This is a consequence of a relatively weak exchange interaction ($|J|/k\approx 0.5$ K). Thus only structural information is required to provide acceptable predictions of the g-value shifts.

ACKNOWLEDGMENTS

One of the authors (R.C.) is also at the Facultad de Bioquímica y Ciencias Biológicas, Universidad Nacional del Litoral, Santa Fe, Argentina. This work was supported by the grants from CONICET PID Nos. 3-905608/85 and 3-098600/88, The Third World Academy of Sciences Grant No. RG86-14, and Fundación Antorchas. The authors are grateful to M. A. Mesa for assistance with some of the experimental work.

APPENDIX

Here we give details on the first-order calculation of the shifts of the resonances with temperature. The role of the anisotropy of the gyromagnetic factors of copper in the dipole-dipole interaction, the anisotropic exchange (symmetric and antisymmetric), and the hyperfine interactions are considered here.

In Cu(*L*-alanine)$_2$, where there are two species of anisotropic copper ions, the total magnetization operator of Eq. (11) should be replaced by

$$\mathbf{M}=-\mu_0\sum_{i=1}^{N}(\vec{\mathbf{g}}_A\cdot\mathbf{S}_{iA}+\vec{\mathbf{g}}_B\cdot\mathbf{S}_{iB}) , \tag{A1}$$

where the summation is over N (a very large number) unit cells of the crystal. Equation (A1) can also be written as

$$\mathbf{M}=-\mu_0(\vec{g}\cdot\mathbf{S}+\overleftrightarrow{G}\cdot\mathbf{s}) , \tag{A2}$$

where

$$\overleftrightarrow{g}=\tfrac{1}{2}(\overleftrightarrow{g}_A+\overleftrightarrow{g}_B)\ , \tag{A3}$$

$$\overleftrightarrow{G}=\tfrac{1}{2}(\overleftrightarrow{g}_A-\overleftrightarrow{g}_B)\ , \tag{A4}$$

$$\mathbf{S}=\sum_i(\mathbf{S}_{iA}+\mathbf{S}_{iB})\ , \tag{A5}$$

and

$$\mathbf{s}=\sum_i(\mathbf{S}_{iA}-\mathbf{S}_{iB})\ . \tag{A6}$$

Within the spirit of the linear-response theory and since we are dealing with a system showing a single exchange-collapsed line, we will assume in the calculation of the correlation function involved in Eq. (9) that

$$\mathbf{M}\approx-\mu_0\overleftrightarrow{g}\cdot\mathbf{S}\ .$$

Thus contributions proportional to $\overleftrightarrow{G}$ of Eq. (A4) were neglected. On the other hand, the Zeeman interaction can be decomposed as

$$\mathcal{H}_z=\mathcal{H}_{z0}+\mathcal{H}'_z\ , \tag{A7}$$

where

$$\mathcal{H}_{z0}=\mu_0\mathbf{S}\cdot\overleftrightarrow{g}\cdot\mathbf{B} \tag{A8}$$

and

$$\mathcal{H}'_z=\mu_0\mathbf{s}\cdot\overleftrightarrow{G}\cdot\mathbf{B}\ . \tag{A9}$$

To the isotropic (Heisenberg) exchange interaction of Eq. (17), we may add anisotropic contributions composed by symmetric and antisymmetric terms,

$$\mathcal{H}_{\rm sym}(i\alpha,j\beta)=\mathbf{S}_{i\alpha}\cdot\overleftrightarrow{J}_{\rm sym}(i\alpha,j\beta)\cdot\mathbf{S}_{j\beta}\ , \tag{A10}$$

$$\mathcal{H}_{\rm ant}(i\alpha,j\beta)=\mathbf{S}_{i\alpha},\overleftrightarrow{J}_{\rm ant}(i\alpha,j\beta)\cdot\mathbf{S}_{j\beta}\ , \tag{A11}$$

where $\overleftrightarrow{J}_{\rm sym}$ and $\overleftrightarrow{J}_{\rm ant}$ are traceless symmetric and antisymmetric tensors. The parameters involved in $\overleftrightarrow{J}_{\rm sym}$ and $\overleftrightarrow{J}_{\rm ant}$ cannot be accurately calculated without going into a first-principles theory. For ions with an orbital contribution to the ground state producing an anisotropy δg of the gyromagnetic factors, Moriya[29] estimated $|J_{\rm ant}|\approx(\delta g/g)J_0$ and $|J_{\rm sym}|\approx(\delta g/g)^2J_0$. Besides these facts, the anisotropic (symmetric) part of the exchange may be handled for many purposes in a way similar to the dipole-dipole interaction. When there are nuclei with spin $I_i=0$, hyperfine interactions $\mathcal{H}_{\rm hf}$ should be considered. In paramagnetic materials the hyperfine interactions are, in general, washed out by the exchange and not observed. However, they may produce sizable effects on the EPR linewidths.[14]

When the interactions $\mathcal{H}'_z$, $\mathcal{H}_{\rm sym}$, $\mathcal{H}_{\rm ant}$, and $\mathcal{H}_{\rm hf}$ are considered, Eqs. (19) and (20) for $\mathcal{H}_0$ and $\mathcal{H}'$ can be rewritten. Now

$$\mathcal{H}_0=\mathcal{H}_{z0}+\mathcal{H}_{\rm ex} \tag{A12}$$

and

$$\mathcal{H}'=\mathcal{H}_{\rm dd}+\mathcal{H}'_z+\mathcal{H}_{\rm sym}+\mathcal{H}_{\rm ant}+\mathcal{H}_{\rm hf}\ . \tag{A13}$$

According to Eqs. (29) and (30), we are to calculate

$$\delta=-\frac{1}{\hbar kT}\frac{\mathrm{Tr}(H_0[\mathcal{H}',S_+]S_0)}{\mathrm{Tr}(S_+S_-)}\ . \tag{A14}$$

This calculation involves several contributions arising from the combinations $(\mathcal{H}_0,\mathcal{H}')$, where $\mathcal{H}_0$ and $\mathcal{H}'$ are given by Eqs. (A12) and (A13). The contributions arising from $(\mathcal{H}_{z0},\mathcal{H}'_z)$ and $(\mathcal{H}_{\rm ex},\mathcal{H}_{\rm dd})$ vanish, as they involve traces of an odd number of spin operators. The contribution arising from $(\mathcal{H}_{\rm ex},\mathcal{H}'_z)$ gives zero as it follows from the exact cancellation of the traces produced by the spins of both A and B sublattices. The contribution of the hyperfine interaction vanish, as it involves traces of operators linear in the nuclear spin components. The effect of the antisymmetric exchange also cancels. Then terms involving $\mathcal{H}_{z0}$, with $\mathcal{H}_{\rm dd}$ or $\mathcal{H}_{\rm sym}$, are the only contributions to Eq. (A14). By choosing a quantization axis $\hat{\mathbf{z}}=\overleftrightarrow{g}\cdot\hat{\mathbf{h}}/g$, where $\hat{\mathbf{h}}=\mathbf{B}/|\mathbf{B}|$ and $g^2=\hat{\mathbf{h}}\cdot\overleftrightarrow{g}\cdot\overleftrightarrow{g}\cdot\hat{\mathbf{h}}$, $\mathcal{H}_{z0}$ takes its diagonal form:

$$\mathcal{H}_{z0}=g\mu_0BS_z\ . \tag{A15}$$

Defining

$$g_T=g_0+\hbar\delta/\mu_0B\ ,$$

one obtains, from Eq. (A14),

$$g_T=g_0-\frac{g_0}{kT}\frac{\mathrm{Tr}(S_z[\mathcal{H}_{\rm dd},S_+]S_-)}{\mathrm{Tr}(S_+S_-)}\ . \tag{A16}$$

In order to consider the effect of the anisotropy of the gyromagnetic factor in the dipole-dipole interaction, it is convenient to write it in terms of mixed tensor operators, taking advantage of their commutation properties with total spin operators.[28] Then a straightforward calculation using Eq. (A16) gives

$$g_T=g_0\left[1-\frac{\mu_0^2}{4kT}[3\hat{\mathbf{z}}\cdot\overleftrightarrow{D}\cdot\hat{\mathbf{z}}-\mathrm{Tr}(\overleftrightarrow{D})]\right]\ , \tag{A17}$$

where, for an infinite crystal,

$$\overleftrightarrow{D}=\frac{1}{2n}\sum_{\alpha,j\beta}\overleftrightarrow{D}(0,\alpha;j,\beta)\ , \tag{A18}$$

n being the number of magnetic ions per unit cell [$n=2$ for Cu(L-alanine)$_2$ and $\alpha,\beta=A,B$] and

$$\overleftrightarrow{D}(i,\alpha;j,\beta)=\frac{1}{(R_{0\alpha,j\beta})^3}(\overleftrightarrow{g}_\alpha\cdot\overleftrightarrow{g}_\beta-3\overleftrightarrow{g}_\alpha\cdot\hat{\mathbf{R}}_{0\alpha,j\beta})(\hat{\mathbf{R}}_{0\alpha,j\beta}\cdot\overleftrightarrow{g}_\beta)\ . \tag{A19}$$

Equations (A17)–(A19) are the basic formulas which have been used to derive the results for simple lattices [Eqs. (33)–(36)], as well as to perform the numerical calculations for Cu(L-alanine)$_2$ described in the text, with results displayed in Table II.

[1]K. Kambe and T. Usui, Prog. Theor Phys. Jpn. **8**, 302 (1952).
[2]M. McMillan and W. Opechowski, Can. J. Phys. **38**, 1168 (1960); **39**, 1369 (1961).
[3]K. Nagata and Y. Tazuke, J. Phys. Soc. Jpn. **32**. 337 (1972).
[4]M. E. Fisher, Am. J. Phys. **32**, 343 (1964).
[5]R. Calvo, J. Appl. Phys. **55**, 2336 (1984).
[6]R. Calvo and M. A. Mesa, Phys. Lett. A **108**, 217 (1985).
[7]A. Fainstein, M. S. thesis, Instituto Balseiro, Bariloche, Argentina, 1986.
[8]P. W. Anderson, J. Phys. Soc. Jpn. **9**, 316 (1954).
[9]R. Kubo and K. Tomita, J. Phys. Soc. Jpn. **9**, 888 (1954).
[10]P. R. Newman, J. L. Imes, and J. A. Cowen, Phys. Rev. B **13**, 4093 (1976).
[11]R. Calvo, M. C. G. Passeggi, M. A. Novak, O. G. Symko, S. B. Oseroff, O. R. Nascimento, and M. C. Terrile, Phys. Rev. B **43**, 1074 (1991).
[12]R. Calvo and M. A. Mesa, Phys. Rev. B **28**, 1244 (1983).
[13]R. Calvo, M. A. Mesa, G. Oliva, J. Zukerman-Schpector, O. R. Nascimento, M. Tovar, and R. Arce, J. Chem. Phys. **81**, 4584 (1984).
[14]R. Calvo, H. Isern, and M. A. Mesa, Chem. Phys. **100**, 89 (1985).
[15]P. R. Levstein, C. A. Steren, A. M. Gennaro, and R. Calvo, Chem. Phys. **120**, 449 (1988).
[16]T. Wakamatsu, T. Hashiguchi, M. Nakano, M. Sorai, H. Suga, and Tan Zhi-Cheng, Chin. Sci. Bull. **34**, 1795 (1990).
[17]P. M. Richards and M. B. Salamon, Phys. Rev. B **9**, 32 (1974).
[18]P. M. Richards, in *Local Properties at Phase Transitions,* Proceedings of the International School of Physics "Enrico Fermi," Course LIX, Varenne on Lake Como, 1976, edited by K. D. Mueller and A. Rigamonti (North-Holland, Elsevier, Amsterdam, 1976), p. 539.
[19]A. Dijkstra, Acta Crystallogr. **20**, 588 (1966).
[20]M. A. Hitchman, L. Kwan, L. M. Engelhardt, and A. H. White, J. Chem. Soc. Dalton Trans. **1987**, 457 (1987). We were unaware of this recent publication when writing Ref. 11.
[21]M. Yokota and S. Koide, J. Phys. Soc. Jpn. **9**, 953 (1954).
[22]R. A. Isaacson, C. A. Lulich, S. B. Oseroff, and R. Calvo, Rev. Sci. Instrum. **51**, 1409 (1980).
[23]S. Bhagavantham, *Crystal Symmetry and Physical Properties* (Academic, London, 1966), Chap. 15.
[24]D. G. McGavin, W. C. Tennant, and J. A. Weil, J. Magn. Reson. **87**, 92 (1990).
[25]A. Abragam, *The Principles of Nuclear Magnetism* (Oxford University Press, London, 1961), Chaps. 4 and 10.
[26]G. Pake, *Paramagnetic Resonance,* 1st ed. (Benjamin, New York, 1962), Chap. 7.
[27]C. Slichter, *The Theory of Magnetic Resonance,* 2nd ed. (Springer, New York, 1980).
[28]M. C. G. Passeggi and R. Calvo, J. Magn. Reson. **81**, 378 (1989).
[29]T. Moriya, Phys. Rev. **120**, 91 (1960).
[30]Y. Natsume, F. Sasagawa, M. Toyoda, and I. Yamada, J. Phys. Soc. Jpn. **48**, 50 (1980).
[31]H. Farach, E. F. Strother, and C. P. Poole, J. Phys. Chem. Solids **31**, 1491 (1970).
[32]Z. G. Soos, K. T. McGregor, T. T. Cheung, and A. J. Silverstein, Phys. Rev. B **16**, 3036 (1977).
[33]R. Calvo and M. C. G. Passeggi, J. Phys. Condens. Matter **2**, 9113 (1990).
[34]K. W. H. Stevens and F. Mehran, J. Phys. C **20**, 5773 (1987).